Available online at www.sciencedirect.com

SciVerse ScienceDirect

Proceedings of the Combustion Institute 34 (2013) 1393–1400

Proceedings of the Combustion Institute

www.elsevier.com/locate/proci

Turbulent premixed flame front dynamics and implications for limits of flamelet hypothesis

Frank T.C. Yuen, Ömer L. Gülder *

Institute for Aerospace Studies, University of Toronto, 4925 Dufferin Street, Toronto, Ontario, Canada M3H 5T6

Available online 24 July 2012

Abstract

Turbulent premixed flames of methane–air and propane–air stabilized on a Bunsen-type burner were studied to investigate the dynamics and structure of the flame front at a wide range of turbulence intensities. The non-dimensional turbulence rms velocity, rms velocity divided by the laminar flame velocity, covered the range from about 3 to 24. The equivalence ratio was varied from 0.6 (0.7 for propane) to stoichiometric. The flame front data were obtained using planar Rayleigh imaging, and particle image velocimetry was used to measure instantaneous velocity field for the experimental conditions studied. The gradients of temperature profiles decreased noticeably with increasing non-dimensional turbulence rms velocity. Flame front curvature statistics indicated that the curvature probability density functions are highly symmetric. Frequency of crossing from negative to positive (and vice versa) curvatures did not show any clear sensitivity to non-dimensional turbulence rms velocity, but decreased by increasing fuel–air equivalence ratio. The product of curvature and diffusivity, a crucial term in the level-set equation proposed for the thin reaction zones regime, was found to be very small as compared to laminar burning velocity, but the product of rms curvature and diffusivity was higher than the laminar burning velocity. Flame surface densities integrated over the flame brush volume did not show any sensitivity to the non-dimensional turbulence rms velocity. Some of the single shot Rayleigh temperature profiles at higher turbulence intensities were radically different than those at lower intensities which are similar to laminar flame profiles. These findings question the validity of the flamelet hypothesis in the thin reaction zones regime where Karlovitz number exceeds unity.

Keywords: Turbulent premixed flames; Validity of flamelet hypothesis; Thin reaction zones regime; Flame surface density; Flame curvature

1. Introduction

The processes involved in turbulent premixed combustion are remarkably complex and some of the factors affecting it are so elusive that our comprehension and description of this important problem is in a confused state. As compared to other combustion problems, turbulent premixed combustion has very few principles whose foundations are firmly established [1]. As a result, we mostly rely on assumptions to describe the physics: many assumptions made in the simulation, and to a certain extend, in experimental analysis of the turbulent premixed flames are based on the flamelet hypothesis. However, the validity of

* Corresponding author. Fax: +1 416 667 7799.
E-mail address: ogulder@utias.utoronto.ca (Ö.L. Gülder).

1540-7489/$ - see front matter © 2012 The Combustion Institute. Published by Elsevier Inc. All rights reserved.
http://dx.doi.org/10.1016/j.proci.2012.06.167

the flamelet hypothesis and the combustion regime where it is applicable are the subjects of much debate. The present study is concerned with the experimental analysis of the rate of propagation of a flame through turbulent premixed reactants, specifically in the regime of thin reaction zones, with an emphasis on the soundness of the flamelet hypothesis.

Through the influence of turbulence, the front of a turbulent premixed flame is subjected to the motions of eddies that leads to an increase in the flame surface area, and the term flame wrinkling is commonly used to describe it. If it is assumed that the flame front would continue to burn locally unaffected by the stretch, then the total turbulent burning rate is expected to increase proportionally to the increase in the flame surface area caused by wrinkling. When the turbulence intensity is high enough such that the stretch due to hydrodynamics and flame curvature would influence the local laminar burning rate, then the actual laminar burning rate should reflect the influence of stretch. It is shown that [2] the front structure of a freely propagating planar flame is insensitive to stretch for equidiffusive flames, i.e. when the Lewis number is unity, such as methane-air mixtures. So the flame front thickness, flame temperature, and burning rate are independent of the hydrodynamic stretch. But in the presence of front curvature, the flame stretch has an effect on the front structure: there is a smoothing effect of curvature on wrinkled flames, and as a consequence the positive curvature tends to reduce local burning rate whereas the negative curvature enhances it.

The planar non-equidiffusive flames, on the other hand, are affected by the hydrodynamic stretch and the direction of this effect depends on the Lewis number, Le, of the deficient reactant. When combined with stretch imposed by flame curvature in wrinkled flames, the tendency to form sharper segments would be enhanced for $\mathrm{Le} < 1$ (e.g., lean hydrogen–air mixtures), and be moderated for $\mathrm{Le} > 1$ (e.g., lean propane–air mixtures) [3]. This means that the degree of wrinkling, and hence the flame surface area, would increase in mixtures with $\mathrm{Le} < 1$ relative to mixtures with $\mathrm{Le} > 1$ as shown by experimental [4] and DNS data [5].

When the turbulence intensity reaches a certain value relative to the laminar burning speed, it seems that the flame surface area increase through wrinkling no longer explains the observed enhancement in the turbulent burning rate with increasing turbulence. Several experimental observations supporting this phenomenon have been reported within the last decade (see e.g. [6–11]). One of the implications of these observations is that the wrinkled laminar flame structure breaks down when the non-dimensional rms velocity, u'/S_L, reaches a certain level. The passive characteristics of the premixed flamelets and their laminar thermal structure are not preserved [6,12,13], and the scalar gradients within the flame front are destroyed by turbulence [8,13]. So there are strong indications that the flamelet assumption used in turbulent premixed flame analysis has a much narrower validity range than currently believed.

Approaches, other than surface area increase, to describe the turbulent flame propagation when the critical u'/S_L level is reached are summarized in the next section. These approaches cover (a) the level-set formulation for the thin reaction zones regime extending the flamelet assumption; (b) the leading edge concept advocated originally in the Soviet literature; and (c) the concept that the small eddies penetrate into the flame front and modify or destroy scalar gradients and enhance heat and mass transport.

2. Background

Adaptation of the G-equation for the "thin reaction zones" regime [14] was to address the non-correlation between flame surface area and the turbulent burning rate when the non-dimensional turbulence rms velocity, u'/S_L, exceeds a critical value. So that the main driver in propagating the turbulent flame would be the curvature, not the perceived increase in the flame surface area. In most practical laboratory flames and in combustion devices, the ratio of integral length scale, Λ, to the laminar flame thickness, δ_L, might range from about 5 to 100. In view of this, transition from wrinkled flame to thin reaction zones regime occurs at about single digit values of u'/S_L. Rigorously, however, the transition is marked by the conditions where the Karlovitz number, Ka, is unity, which is known as Klimov–Williams criterion [1], indicating that the wrinkled laminar flame structure exists if the Reynolds number based on Kolmogorov length scale, R_η, is larger than u'/S_L. Markstein [15] originally formulated the level set equation for the premixed flame propagation that is now known as the G-equation:

$$\frac{\partial G}{\partial t} + v \cdot \nabla G = S_L |\nabla G| \tag{1}$$

Equation (1) was modified to represent the physics of the flame propagation within the thin reaction zones regime. In the theory for the thin reaction zones regime [14] the propagation speed of the instantaneous flame is given by $s_\kappa = D\kappa$, where D is the diffusivity and κ is the local flame curvature. It is argued that this value is much higher than the laminar burning velocity in this regime. The proposal that s_κ should be used instead of the laminar burning velocity in the thin reaction zone regime is based on the two-dimensional DNS data [16]. The proposed level set equation for the thin reaction zones regime is a modification of the G-equation, given as [14]:

$$\frac{\partial G}{\partial t} + v \cdot \nabla G = S_{L,s}|\nabla G| - D\kappa|\nabla G| \quad (2)$$

where $S_{L,s} = S_n + S_r$, and S_n and S_r are contributions due to normal diffusion and reaction to the displacement speed of the thin reaction zone. However, $S_{L,s}$ is the same order of magnitude as the laminar burning velocity. Therefore the observed high turbulent burning rates are accounted for by the $D\kappa$, in the second term on the right hand side of Eq. (2). It is conjectured that the magnitude of $D\kappa$ will be much greater than the laminar burning velocity so that the modified G-equation would be able to represent premixed turbulent combustion in the thin reaction zones regime.

One of the concepts originally discussed in Soviet literature in 1970s is the propagation of the turbulent flame by the leading edges (or leading points) of the flame extending into the unburned mixture [17]. The characteristics of the positive curvatures of the flame front then determine the rate of flame propagation. The development of this concept was attributed to Zeldovich [18] and the original idea behind it seems to be proposed by Baev and Tret'yakov [19]. So it is proposed that, at least in lean flames, the influence of negative curvatures is minimal whereas the influence of positive curvature dominates the propagation rate. Details of this concept are discussed by Sabel'nikov and Kuznetsov [20] as well as by Kuznetsov [18], and a schematic is shown in Fig. 1. Leading points, shown by arrows on the lower part of the χ-axis, are the drivers for the flame propagation irrespective of the negatively curved parts of the flame sheet above the χ-axis.

The influence of turbulence on the inner structure of a premixed flame front is not trivial even in the wrinkled flamelets regime [18]. Ronney and Yakhot [21] conclude that the effect of scales smaller than the laminar flame front thickness is probably significant for most flames at sufficiently high turbulence intensities. Detailed measurements of O'Young and Bilger [12] show that small high-turbulence intensity eddies, comparable to the thermal flame front thickness in size, have a strong convective effect on the preheat zone, broadening of the thermal flame front. In addition, as turbulence increases, the value of the conditional mean of the scalar dissipation departs significantly from that of a laminar flame [12]. It is shown in [6,8–10] that when the non-dimensional turbulence intensity, u'/S_L, exceeds about 6–7, the flame surface area increase estimated by the fractal analysis or flame surface density approaches does not explain the observed increases in the turbulent burning velocity. One of the potential contributors to the flame propagation is the enhancement of the transport within the flame front by small size eddies that could penetrate into the preheat layer. An expression was derived in [8] to estimate the contribution of flame front alteration, as a consequence of the small scale turbulent eddies that may penetrate into the preheat layer of the premixed flame front, to the flamelet burning velocity. The derivation was based on that (a) there is experimental evidence of flame front alteration by active eddies penetrating into the preheat layer and enhancing the transport, (b) these active eddies have a characteristic size approximating the Taylor microscale, and (c) within the turbulence cascade the volume occupied by a certain size eddy and its velocity obey power-law relationships (i.e. structure functions), dictated by the intermittency of the turbulent field.

In this paper, experimental results obtained by 2D Rayleigh scattering in lean and stoichiometric turbulent premixed flames are analyzed to address the question of the validity domain of flamelet assumption. The turbulence intensities covered the regimes of wrinkled and thin reaction zones. The results are discussed with respect to the three approaches summarized above.

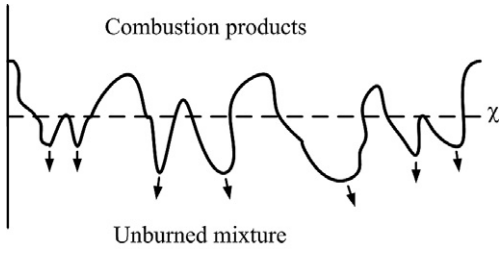

Fig. 1. Schematic description of the leading edge (or points) concept of flame propagation. Leading points, shown by arrows on the lower part of the χ-axis, are the drivers for the flame propagation. Adapted from [18].

3. Experimental methodology

Experimental setup, the method of measurements, and the data analysis used in the current work were presented in detail previously [11,22]. Here a brief description will be given. The burner is a Bunsen type circular burner with a nozzle diameter of 11.2 mm.

Flame front images were captured using planar Rayleigh scattering [23–25]. This setup consisted of a third harmonic (355 nm) Nd:YAG laser working at an energy level of 305 mJ/pulse and a frequency of 10 Hz; a set of beam-shaping optics through which the laser beam passed to produce a laser sheet of 60 mm high and 150 μm thick; an intensified CCD camera with an array size of 1024×1280 pixels positioned at 90° to the scattered light, and equipped with a 4.1 f-number 94 mm focal length camera objective. With this setup, a capture area of 57×46 mm and a

resolution of 45 μm/pixel were achieved. The signal to noise ratio for the products is about 14.3, and for the reactants 23.8. This is found by calculating the ratio between the mean and standard deviation for an area of 2500 pixels in the product and reaction regions of the flame. Typical Rayleigh scattering intensity is about 260 counts for reactant pixels and 72 for product pixels. However, with this arrangement of the optical layout, it was necessary to divide the flame into three sections along the flame centerline, and images were captured for three sections separately. Each section of the flame has a height of 44 mm and width of 22 mm. The centers of the sections are 66.5, 96.5, and 121.5 mm above the burner rim. More than 300 images were captured for each experimental condition.

The maximum resolution of the Rayleigh imaging system was found using the Contrast transfer function (CTF) which corresponds to 22 line-pairs/mm at CTF of 10%. Thus, the limiting resolution for the Rayleigh scattering measurements would be the laser sheet thickness which is 150 μm. Details of the Rayleigh image analysis and extraction of the flame front thickness, curvature, and flame surface density information are described in [11].

Particle image velocimetry (PIV) was used to measure instantaneous velocity field for the experimental conditions studied. The PIV experiment was conducted separately from the Rayleigh scattering experiments. The system consisted of a double-pulsed second harmonic (532 nm) Nd:YAG laser working at an energy level of 50 mJ/pulse and a frequency of 15 Hz; a CCD camera with an array size of 1600 × 1186 pixels and equipped with a 2.8 f-number 60 mm focal length camera objective. This optical setup was used to capture the flow condition above the nozzle exit with a view area of 11.6 × 15.7 mm and a resolution of 9.8 μm/pixel. The time separation between the two laser pulses was 10 μs. The submicron oil droplets were generated by a nebulizer as seeding particles. The image scale factor was 1.326; the interrogation region was 32 × 32 pixels; and the pixel pitch was 5.56 μm. The multiplication of these terms gives the actual PIV resolution which is about 0.24 mm. This is the smallest velocity structure that can be resolved which is smaller than the Taylor length scale. The length scales were estimated by using the velocity field data from the PIV measurements which yielded fluctuating rms velocity u'. The auto-correlation functions of u' were calculated along the length of the image. The integral length scales were found by integrating the auto-correlation functions to where they first crossed zero. The Taylor length scales were estimated by constructing an osculating parabola for the auto-correlation function. The distance to which the parabola crosses zero is the Taylor length scale.

4. Results and discussion

4.1. Flame front thermal structure

The Rayleigh scattering images were processed to provide instantaneous temperature gradients at progress variable $c = 0.5$ and 0.3, where $c = (T - T_u)/(T_b - T_u)$. T, T_b, T_u are the instantaneous, burned gas, and unburned gas temperatures, respectively. Temperature gradient probability density functions (pdf) had a Gaussian shape, an example of which is shown in Fig. 2. Temperature gradient data, plotted in Fig. 3, are the peaks of the temperature gradient pdfs at each experimental condition at $c = 0.3$ for methane and propane flames. Error bars represent plus and minus one standard deviation of the corresponding temperature gradient pdf, Fig. 3. The total error, on the other hand, in evaluating the temperature gradient from Rayleigh images was found to be about 11–13% [26]. Temperature gradients show a definite decreasing trend with increasing non-dimensional turbulence velocity which means that the thermal flame thickness increases with increasing turbulence rms velocity. However, the decrease in temperature gradient levels off when u'/S_L reaches about 10, Fig. 3. In both methane and propane flames, thermal flame thickness obtained from the gradients of the temperature profiles increases with increasing turbulence intensity irrespective of progress variable at which the data are evaluated.

4.2. Flame front curvature

Most recent 3D DNS results [27] show that the mean flame front curvature in turbulent premixed flames is negative and deviation from the zero mean increases with increasing turbulence intensity. Experimental data, on the other hand, indicate that with increasing turbulence the curvature distribution assumes almost a perfect symmetrical pdf centered at zero [22,28], indicating

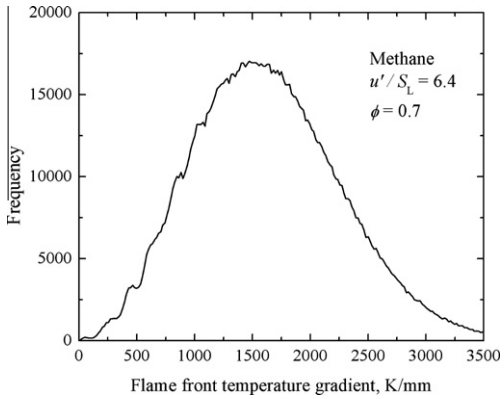

Fig. 2. An example of the temperature gradient pdf.

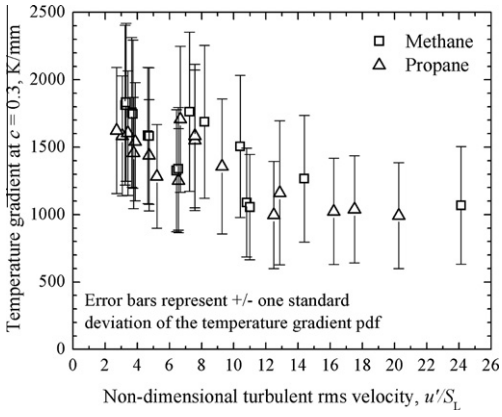

Fig. 3. Variation of the peaks of the temperature gradient pdfs with non-dimensional turbulent rms velocity.

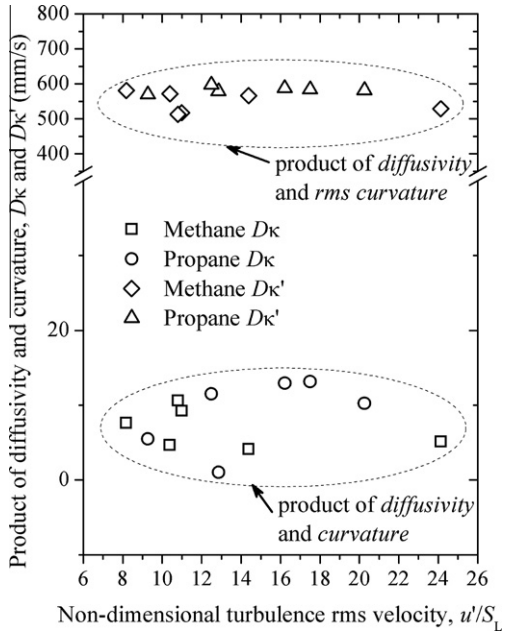

Fig. 4. Product of curvature and diffusivity, and the product of rms curvature and diffusivity at various turbulence intensities.

that the positive and negative curvatures exist at the flame front with an equal probability. Thin reaction zones formulation in Eq. (2) is based on the results of 2D DNS calculations which show that the mean flame front curvature is negative and deviation from the zero increases with increasing turbulence intensity [16]. The variation of the term $D\kappa$ in Eq. (2), evaluated using the curvature data and diffusivities calculated at 1800 K, with u'/S_L is shown in the lower part of Fig. 4. If one evaluates the rms value of the curvature, κ', then the product of diffusivity and the rms curvature, $D\kappa'$, reaches values that exceed the laminar flame velocities as shown in the upper part of Fig. 4.

Note that $D\kappa$ data are presented for conditions where the non-dimensional turbulence rms velocity is larger than about 8. The magnitude of the term $D\kappa$ is much smaller than the laminar burning velocity for both methane and propane flames. These results question the validity of extending the level set formulation, developed for passive surface thin flame propagation, into the thin reaction zone regime by modifying the local flame propagation by the term $D\kappa$ in addition to laminar burning velocity. On the other hand, if the $D\kappa$ term in Eq. (2) is replaced by $-|D\kappa'|$, then it makes a non-trivial contribution to the flame propagation velocity. However, this exercise is somewhat similar to assuming that the "leading points" concept, discussed in the Background section, is the mode of operation in turbulent premixed flames, and the rms curvature somehow captures the physics of "leading points" concept. One caution is that, as can be deduced from the discussion on leading points concept in literature, the inner structure of the turbulent flame front is assumed to be significantly influenced by turbulence and the preferential diffusion plays an important role [18,20] in the leading points concept, whereas in Eq. (2) the main assumption is that the flame front, specifically the reaction zone, is still a passive surface.

An alternative measure of the flame front curvature is the statistics of occurrence of zero curvature points, i.e. transitions from negative to positive curvatures, along the flame contours. Since the curvature pdfs are almost symmetrical around zero, zero curvature points may provide information on the degree of wrinkling as a function of equivalence ratio and u'/S_L. For each flame condition, 300 flame images were processed to determine the zero curvature statistics of the instantaneous flame surfaces. Leaner mixtures exhibit larger number of zero crossings, Fig. 5. Frequency of occurrences in Fig. 5 were normalized by the total number of images in each set. The turbulence intensity sensitivity of the zero crossings, however, is not clear cut from the data shown in Fig. 5. Presenting the data as a function of u'/S_L does not indicate any conclusive sensitivity on the turbulence rms velocity, Fig. 6. Similar behavior to that of methane was observed for propane flames. These observations indicate a defiency in the formulation of the modified level-set equation for the thin reactions zone regime (Eq. (2)).

4.3. Flame surface density

It can be shown that the non-dimensional turbulent burning velocity is proportional to the flame surface density integrated over the flame

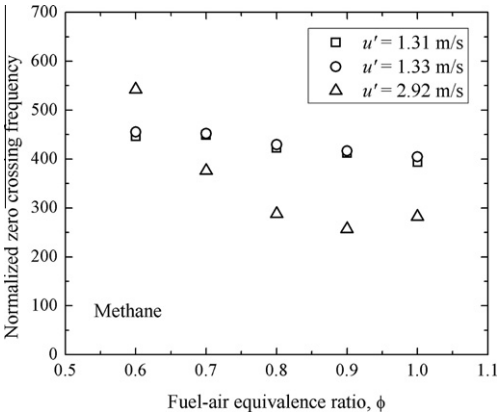

Fig. 5. Frequency of occurrence of zero curvature points along the flame contours as a function of fuel–air equivalence ratio in methane flames.

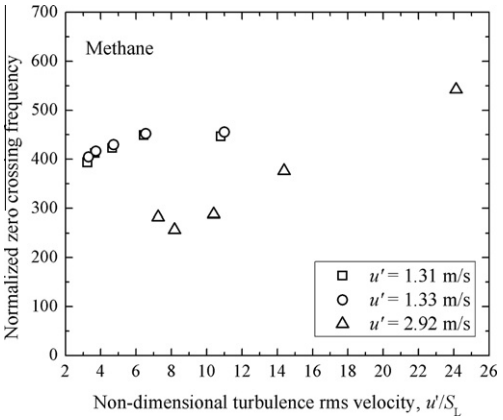

Fig. 6. Frequency of occurrence of zero curvature points along the flame contours as a function of non-dimensional turbulence intensity in methane flames.

brush volume (see for example [29]), i.e. $S_T/S_L = \int \sum dV/A_0$. The flame surface density data obtained in this study were used to evaluate the integrated flame surface densities for methane and propane flames. Integrated flame surface densities are plotted, along with turbulent flame burning velocities determined experimentally, as a function of non-dimensional turbulence rms velocity in Figs. 7 and 8. Burning velocities were determined using the procedure outlined in [6,10]. Integrated flame surface density shows no clear dependence on the turbulence intensity for the turbulent flame conditions studied in the present work. The observations that the integrated flame surface density do not change with the non-dimensional turbulence intensity have some serious implications. Experimental measurements on turbulent premixed flames have shown that the turbulent burning velocity increases with

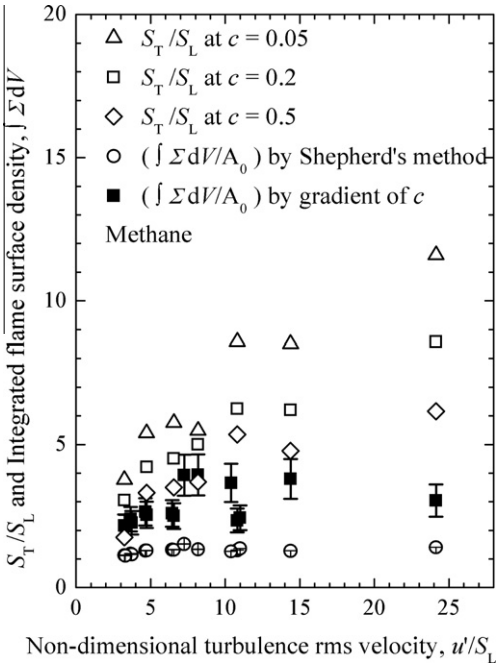

Fig. 7. Variation of integrated flame surface density and non-dimensional turbulent burning velocity of premixed turbulent methane flames with non-dimensional turbulence rms velocity. Direct measurements refer to burning velocities determined using the procedure outlined in [6,10]. Shepherd's method is detailed in [36]. Error bars on integrated flame surface densities represent systematic and random errors and are about 15–20% [26].

increasing turbulence. Turbulent burning velocity data from the current measurements also show an increasing trend with increasing non-dimensional turbulence rms velocity as shown in Figs. 7 and 8. The turbulent burning velocity S_T increases as the turbulence intensity is increased. Thus the integrated flame surface density is expected to increase with increasing u'/S_L in accordance with the assumed relationship between the burning rate and the flame surface area, however, it does not show any evidence of significant dependence on the flow turbulence.

4.4. Non-flamelet flame structure

Single shot Rayleigh temperature profiles for five cases are shown in Fig. 9, where the temperature is plotted against a spatial coordinate normal to the flame surface. Temperature profile M9, taken from the flame with $u'/S_L = 6.5$, is similar to a laminar flame temperature profile, whereas profiles of M15, taken from the flame with $u'/S_L = 24$, in Fig. 9, however, deviate significantly from that of M9. The temperature bulges in front of the preheat zone in M15 profiles are similar to that reported in [30]. What is significant is the

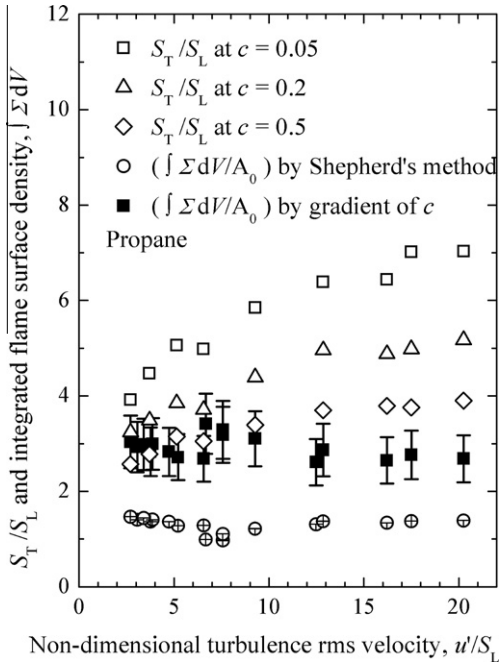

Fig. 8. Variation of integrated flame surface density and non-dimensional turbulent burning velocity of premixed turbulent propane flames with non-dimensional turbulence rms velocity. Direct measurements refer to burning velocities determined using the procedure outlined in [6,10]. Shepherd's method is detailed in [36]. Error bars on integrated flame surface densities represent systematic and random errors and are about 15–20% [26].

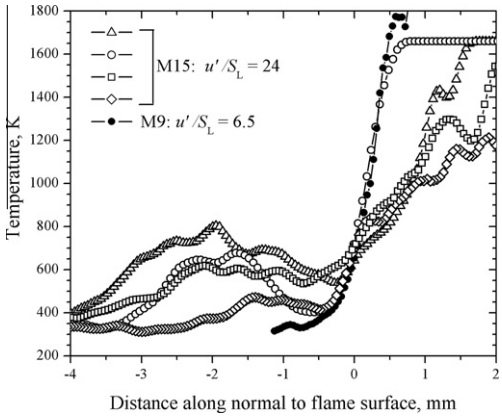

Fig. 9. Selected temperature profiles (filtered) from single-shot Rayleigh measurements.

change in thermal structure in the reaction zone of the flame, Fig. 9. These temperature profiles validate the findings showing that the fine scale turbulence and strain modifies or destroys the scalar gradients within the flame front [12,13].

Chen and Mansour [31] observed an increase in the flame thickness with increasing turbulence intensity. They attributed this broadening to the penetration of smaller eddies into the preheat zone and enhancing scalar transport. They claimed that the chemical reaction zone would not be affected and still remains relatively thin. However, the temperature profiles shown in Fig. 9 question their assertions.

The current experimental results and their analysis cast doubt on the validity of the flamelet hypothesis in the thin reaction zones regime. Further, flamelet hypothesis is not supported by the extensive amount of experimental data [6–13,32] when the non-dimensional turbulent rms velocity exceeds a certain limit. For practical purposes, these observations limit the validity of the flamelet hypothesis to conditions where the Reynolds number based on the Kolmogorov length scale is larger than the non-dimensional turbulent rms velocity. Original criterion proposed by Klimov [33,34] indicates that when the ratio of characteristic chemical time to turbulence time exceeds unity (i.e, $Ka \gg 1$), *surface combustion* is no longer possible. To the current authors' knowledge, there are not any experimental data that directly supports the validity of the flamelet hypothesis unambiguously beyond the Klimov's criterion when $Ka \gg 1$.

Buschmann et al. [35] report that for flames with $1 < Ka < 16.8$, the mean flame front thickness is significantly different than laminar calculations, whereas for $Ka < 1$ measured flame thicknesses are similar to laminar calculations. At $Ka > 5$, they observed strong deviations from flamelet structure and suggested that $Ka \approx 5$ might be understood as the limit to the flamelet regime. Our results are in qualitative agreement with these observations [35]. However, results discussed in this paper are in contradiction to the DNS results that advocate much wider regime for the validity of flamelet assumption, see e.g. [37].

Although the current experimental work is 2D, the justification for its relevance to 3D, and the errors involved can be found in [11,38].

5. Concluding remarks

The measurements of the turbulent premixed flame front characteristics presented here for methane and propane flames at non-dimensional turbulence intensities from 3 to 24 lead to the following conclusions:

1. Flame surface area, reported as flame surface density integrated through the flame brush volume, does not keep growing with turbulence intensity beyond a certain non-dimensional turbulence rms velocity.

2. Flame front curvature is mostly symmetric around zero, especially at high turbulence intensities. Numerical value of the product of curvature and diffusivity is much smaller than the laminar burning velocity, and does not contribute to flame propagation per the level-set equation proposed for the thin reaction zones regime.
3. Fine scale turbulence modifies or destroys the temperature gradients within the flame front enhancing the transport of heat and species.
4. Experimental findings question the validity of the flamelet hypothesis, and it was argued that the flamelet hypothesis is not valid when the Karlovitz number $Ka \gg 1$.

Acknowledgements

This work has been supported by grants (CRO and Discovery) from the Natural Sciences and Engineering Research Council (NSERC).

References

[1] F.A. Williams, *Combust. Flame* 26 (1976) 269–270.
[2] C.K. Law, C.J. Sung, G. Yu, R.L. Axelbaum, *Combust. Flame* 98 (1994) 139–154.
[3] C.K. Law, *Combustion Physics*, Cambridge University Press, New York, 2006 (Chapter 10).
[4] P.J. Goix, I.G. Shepherd, *Combust. Sci. Technol.* 91 (1993) 191–206.
[5] N. Chakraborty, R.S. Cant, *Combust. Flame* 156 (2009) 1427–1444.
[6] Ö.L. Gülder, G.J. Smallwood, R. Wong, D.R. Snelling, R. Smith, B.M. Deschamps, J.-C. Sautet, *Combust. Flame* 120 (2000) 407–416.
[7] Y.-C. Chen, R.W. Bilger, *Combust. Flame* 131 (2002) 400–435.
[8] Ö.L. Gülder, *Proc. Combust. Inst.* 31 (2007) 1369–1375.
[9] E. Cintosun, G.J. Smallwood, Ö.L. Gülder, *AIAA J.* 45 (2007) 2785–2789.
[10] Ö.L. Gülder, G.J. Smallwood, *Combust. Sci. Technol.* 179 (2007) 91–206.
[11] F.T.C. Yuen, Ö.L. Gülder, *Proc. Combust. Inst.* 32 (2009) 1747–1754.
[12] F. O'Young, R.W. Bilger, *Combust. Flame* 109 (1997) 682–700.
[13] G. Hartung, J. Hult, C.F. Kaminski, J.W. Rogerson, N. Swaminathan, *Phys. Fluid* 20 (2008) 035110–035116.
[14] N. Peters, *Turbulent Combustion*, Cambridge University Press, Cambridge, UK, 2000, p. 106.
[15] G.H. Markstein, in: G.H. Markstein (Ed.), *Nonsteady Flame Propagation*, Pargamon Press, 1964, pp. 5–14.
[16] N. Peters, P. Terhoeven, J.H. Chen, T. Echekki, *Proc. Combust. Inst.* 27 (1998) 833–839.
[17] N. Lipatnikov, J. Chomiak, *Prog. Energy Combust. Sci.* 31 (2005) 1–73.
[18] V.R. Kuznetsov, *Center for Turbulence Research Annual Research Briefs 1992*, 1992, pp. 443–453.
[19] V.K. Baev, P.K. Tret'yakov, *Combust. Expl. Shock Waves* 4 (3) (1968) 208–214.
[20] V.R. Kuznetsov, V.A. Sabel'nikov, *Turbulence Combustion*, Hemisphere, 1990 (Chapter 6).
[21] P.D. Ronney, V. Yakhot, *Combust. Sci. Technol.* 86 (1992) 31–43.
[22] F.T.C. Yuen, Ö.L. Gülder, *AIAA J.* 47 (12) (2009) 2964–2973.
[23] A.C. Eckbreth, *Laser Diagnostics for Combustion Temperature and Diagnostics*, second ed., Gordon and Breach Publishers, Kent, UK, 1996.
[24] R.W. Dibble, R.E. Hollenbach, *Proc. Combust. Inst.* 18 (1981) 1489–1499.
[25] R.B. Miles, W.R. Lempert, J.N. Forkey, *Meas. Sci. Technol.* 12 (2001) R33–R51.
[26] F.T.C. Yuen, Ph.D. thesis, University of Toronto, 2009.
[27] I. Han, K.Y. Huh, *Proc. Combust. Inst.* 32 (2009) 1419–1425.
[28] A. Soika, F. Dinkelacker, A. Leipertz, *Combust. Flame* 132 (2003) 451–462.
[29] J.F. Driscoll, *Prog. Energy Combust. Sci.* 34 (2008) 91–134.
[30] C. Kortschik, T. Plessing, N. Peters, *Combust. Flame* 136 (2004) 43–50.
[31] Y.-C. Chen, M.S. Mansour, *Proc. Combust. Inst.* 27 (1998) 811–818.
[32] Y.-C. Chen, *Proc. Combust. Inst.* 32 (2009) 1771–1777.
[33] A.M. Klimov, *Zhur. Prikl. Mekh. Tekhn. Fiz.* 3 (1963) 49–58.
[34] A.M. Klimov, V.N. Lebedev, *Combust. Expl. Shock Waves* 19 (5) (1983) 540–542.
[35] A. Buschmann, F. Dinkelacker, T. Schafer, M. Schafer, J. Wolfrum, *Proc. Combust. Inst.* 26 (1996) 437–448.
[36] I.G. Shepherd, *Proc. Combust. Inst.* 26 (1966) 373–379.
[37] T. Poinsot, S. Candel, A. Trouvé, *Prog. Energy Combust. Sci.* 21 (1996) 531–576.
[38] Y. Zhang, K.N.C. Bray, B. Rogg, *Combust. Sci. Technol.* 137 (1998) 347–358.